BOLETIN DE LA SOCIEDAD ESPAÑOLA DE
Cerámica y Vidrio
www.elsevier.es/bsecv

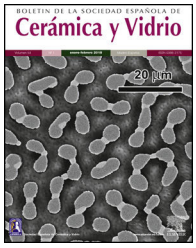

Exploring the diversity of clays: Impacts of temperature on physicochemical changes, mechanical characteristics, and permeability, and their relevance to membrane applications

Khadija Elataoui[a], *Mohamed Amine Harech*[a,*], *Hajar Qobay*[a], *Noureddine Elbinna*[a], *Hakima Aouad*[a], *Mohamed Waqif*[b], *Latifa Saadi*[b]

[a] *Laboratory of Materials Science and Processes Optimization, Department of Chemistry, Faculty of Sciences Semlalia Marrakech, Cadi Ayyad University, Marrakech, Morocco*
[b] *Laboratory Innovative Materials, Energy and Sustainable Development Laboratory, Department of Chemistry, Marrakech, Morocco*

ARTICLE INFO

Article history:
Received 19 January 2024
Accepted 16 July 2024
Available online 30 July 2024

Keywords:
Membranes
Characterization
Thermal treatment
Red clay
Gray clay

ABSTRACT

This study investigates the characterization of two clays obtained from the Safi and Fez regions, focusing on their analysis for filtration membrane applications. Various analytical techniques were employed, including chemical composition analysis, elemental analysis, mineralogical characterization, carbonate content determination, color assessment, plasticity evaluation, thermal treatment analysis (DTA-TG), mineralogical transformation study, fusion tests, membrane tests, and scanning electron microscopy (SEM).

The results reveal significant differences between the two clays regarding their chemical composition. The red clay exhibits a mineralogical composition comprising quartz, calcite, dolomite, hematite, illite, and kaolinite, whereas the gray clay contains quartz, calcite, dolomite, illite, talc, and montmorillonite. Furthermore, upon thermal treatment, both clays exhibit changes in their physical properties.

Despite the decrease in porosity and water absorption, as well as the increase in compression strength for both clays, the permeability of the grey clay increases, unlike the red clay, which exhibits a constant permeability beyond 1000 °C.

These findings highlight the diversity and industrial significance of clays from the Safi and Fez regions for filtration membrane applications. The contrasting properties of red and gray clays provide insights into their potential utilization in different industries. Exploring these clays' behavior can lead to better filtration membranes and new industrial applications.

* *Corresponding author.*
E-mail address: mharech@gmail.com (M.A. Harech).
https://doi.org/10.1016/j.bsecv.2024.07.001

Explorando la diversidad de las arcillas: impacto de la temperatura en cambios fisicoquímicos, características mecánicas y permeabilidad, y su relevancia en aplicaciones de membranas

Palabras clave:
Membranas
Caracterización
Tratamiento térmico
Arcilla roja
Arcilla gris

RESUMEN

Este estudio investiga la caracterización de dos arcillas obtenidas de las regiones de Safi y Fez, centrándose en su análisis para aplicaciones de membranas de filtración. Se emplearon diversas técnicas analíticas, incluyendo análisis de composición química, análisis elemental, caracterización mineralógica, determinación del contenido de carbonato, evaluación del color, evaluación de plasticidad, análisis térmico (DTA-TG), estudio de transformación mineralógica, pruebas de fusión, pruebas de membrana y microscopía electrónica de barrido (SEM).

Los resultados revelan diferencias significativas entre las dos arcillas en cuanto a su composición química. La arcilla roja presenta una composición mineralógica que incluye cuarzo, calcita, dolomita, hematita, illita y caolinita, mientras que la arcilla gris contiene cuarzo, calcita, dolomita, illita, talco y montmorillonita. Además, tras el tratamiento térmico, ambas arcillas experimentan cambios en sus propiedades físicas.

A pesar de la disminución en la porosidad y absorción de agua, así como el aumento en la resistencia a la compresión para ambas arcillas, la permeabilidad de la arcilla gris aumenta, a diferencia de la arcilla roja, que muestra una permeabilidad constante más allá de los 1000 °C.

Estos hallazgos resaltan la diversidad y la importancia industrial de las arcillas de las regiones de Safi y Fez para aplicaciones de membranas de filtración. Las características de las arcillas rojas y grises proporcionan información sobre su posible utilización en diferentes industrias. Explorar el comportamiento de estas arcillas puede conducir a mejores membranas de filtración y nuevas aplicaciones industriales.

Introduction

Morocco has diverse clay deposits, each with special qualities appropriate for industrial and ceramic uses [1,2]. These clays, derived from dissimilar geological formations, have distinct properties, including flexibility, heat resistance, and chemical composition, making them valuable for different industrial uses [3–5]. Moroccan clays are in high demand because of their extraordinary flexibility in the pottery industry [6]. They are perfect for making tiles, pottery, and other ceramic products since they can be easily molded and molded into complicated shapes [7,8]. The chemical composition of Moroccan clays also contributes to their industrial value [9,10]. These clays contain minerals and elements, including silica, aluminum, iron oxide, and oligo-elements. These components enhance the distinctive qualities of clays, making them suitable for various industrial applications [11–14]. For instance, iron oxide gives some clays a distinctive reddish hue highly desired in the ceramics industry for its aesthetic appeal [15–17].

The coastal city of Safi, Morocco, has large deposits of excellent-quality red clay. Safi's clay deposits are distinguished by their purity, consistency, and bright red color, which results from iron oxide [18]. These characteristics make it a valuable resource of industrial importance. Safi red clay is widely used in the industry to produce ceramic tiles, bricks, and handicraft products. Safi red clay is wear-resistant, making it suitable for indoor and outdoor applications [19–21]. The availability of high-quality clay reserves in Safi has contributed to the growth of the local ceramics industry, facilitating economic development and establishing Morocco as a global competitor.

A city renowned for its cultural heritage, Fez is home to large reserves of gray clay [5,8,22]. The deposits of gray clay of Fez have unique properties that make them suitable for various applications [22]. The specific characteristics of gray clay, such as particle size and chemical composition, make it ideal for specific industrial applications. Its use in refractory materials contributes to the heat resistance and structural integrity required in the metallurgy and cement manufacturing industries [23].

In recent years, the use of clays for the preparation of filtration membranes has received considerable attention [24,25]. Clays, including the ones found in Morocco, have fine particles and a porous structure, which makes them suitable for creating membranes with high surface area and selective permeability [26–28]. Modifying the clay's properties by incorporating pore-forming agents and heat treatment makes it possible to adapt the membranes to specific filtration applications [29]. The technology of clay-based membranes provides several advantages for filtration applications: they are cost-effective, readily available, and environmentally friendly compared to traditional filtration materials [30].

Clay-based membranes' scalability makes them a promising solution for large-scale filtration processes in water treatment, pharmaceuticals, and food processing industries. In addition, its unique properties, such as its high surface area and cation exchange capacity, help improve the performance of filtration membranes [31]. The fineness and porous structure of clays facilitate the retention and removal of contaminants, thus ensuring efficient filtration processes. Furthermore, the ability to modify the properties of clays allows for the optimization of membrane characteristics such as permeability, selectivity, and mechanical strength to meet specific filtration requirements.

Moroccan clays have various properties that contribute to their importance for industrial and ceramic applications. The red clay of Safi and the gray clay of Fez are particularly important because of their reserves and suitability for specific industries. Moreover, using these clays to prepare filtration membranes offers a promising solution for efficient and durable systems. The detailed characterization of these clays allows us to understand all the phenomena that will take place during the preparation of the membranes, and it will also provide valuable information on their filtration performances, allowing the development of advanced filtration technologies in Morocco and the world.

Material and methods

Raw materials and pretreatment

The two clays investigated in the study have been sourced from two distinct regions in Morocco. The first clay was obtained from Safi (red clay), a coastal city in western Morocco, while the second clay was procured from Fez (gray clay), located in the country's northern central part. The clay samples were collected and then prepared for analysis. This entailed drying the samples and grinding them into a fine powder, which was then passed through a 100 μm sieve to remove impurities and coarse particles. The resulting powder was subsequently utilized for all subsequent analyses.

Powder characterization techniques

We analyzed the chemical composition of each clay using X-ray fluorescence spectroscopy (XRF). This technique allowed us to determine the elemental composition of each sample, including significant elements. A Panalytical ZETIUM X-ray fluorescence instrument (Malvern Panalytical, Malvern, U.K.) was used in this study.

X-ray powder diffraction was also used to examine the mineralogical makeup of the raw materials and ceramics heated to 900, 1000, and 1100 °C (XRD). The materials were crushed into a fine powder, and Rigaku SmartLab's CuK radiation diffractometer was used to gather data across a range of 5–60 2Theta by degrees with a 0.04-degree step size (Tokyo, Japan). The PDF 2004 database's diffractogram was compared to diffraction peaks to identify minerals.

Heavy metals were determined using inductively coupled plasma optical emission spectroscopy (ICP-AES, Ultima Expert, Horiba Inc., Toronto, Ontario, Canada). The samples were made as follows: in Teflon digesting vessels, 20 mg of the clay sample were precisely weighed, and 1 mL of a concentrated HNO_3 solution and 4 mL of an HF solution were added (Sigma-Aldrich, St. Louis, Missouri, USA). For 75 min, the samples were heated in a microwave. The colorless solutions were quantitatively transferred to 100 mL volumetric flasks after cooling, and the volume was then filled to the desired level with deionized water.

The thermal analyzer is used to assess the thermal behavior of both clays (DTA-TG) (STA PT 1600, Linseis, Selb, Germany). At a heating rate of 10 °C/min, the results were achieved in the air between 25 and 1050 °C. Using this method, we could ascertain the temperatures at which the clays underwent mineralogical transition and weight loss.

Using a Mastersizer 2000 laser particle size analyzer, the size distribution of the clay particles was determined (Malvern Panalytical, Malvern, U.K.). Then, the oversized agglomerates were broken up by sonicating the solution for 1 min after adding 40 mg of the powder to 40 mL of water. The plasticity limit is evaluated according to the Moroccan standard Nm iso 17892-12.

The Bernard technique is a good choice for quickly determining the carbonate content % [11]. Five grams of clay powder were combined with 10 mL of concentrated hydrochloric acid (Sigma-Aldrich, Missouri, United States) in a graduated cylinder after it was first filled with water (1N). The interaction between the acid and clay particles forced water out of the graduated cylinder, which created CO_2. The sample's carbonate quantity was then determined by directly weighing the gas emitted.

Preparation of clay ceramic membrane

In this study, we aimed to investigate precisely the physicochemical, mechanical properties, and workability of the two different types of clays as filtration membranes. We prepared three different sizes of pellets red and gray clay, to achieve this. The powders were carefully prepared by weighing the desired amount of red and gray clay with a precision balance. Next, the pellets made from clay were used in a dry method. Finally, the powder was axially compressed by 2.4 tons to produce pellet (a) and by one ton for pellets (b) and (c), which were then heated to different temperatures.

- (a): 20 mm in diameter and 2 mm in thickness.
- (b): 13 mm in diameter and 17 mm in thickness.
- (c): 13 mm in diameter and 1.5 mm in thickness.

The heat treatment was performed in an electric furnace (LH 15/12 System, Nabertherm Lilienthal, Germany). The thermal cycle is explained below:

The target temperatures of 900, 1000, and 1100 °C were attained by applying a temperature ramp of 5 °C/min. Following 2 h at the predetermined temperature, the samples were allowed to cool naturally while the oven was turned off. Fig. 3 shows the effect of temperature and composition on sintered pellets.

Table 1 – Chemical composition of red and gray clay.

Oxides	SiO_2	Al_2O_3	Fe_2O_3	MgO	MnO	CaO	K_2O	Na_2O	TiO_2	P_2O_5	LOI
Red clay	52.76	17.34	5.95	2.63	0.03	3.84	4.72	0.42	–	0.17	11.6
Gray clay	47.17	9.54	4.13	4.08	0.035	14.16	1.26	0.78	0.55	–	16.27

Characterization of clay ceramic membrane

The Archimedes technique was used to calculate the samples' bulk density, open porosity, and water absorption values as part of the investigation into the physical characteristics of the samples. First, the ceramic pieces were submerged in water for 24 h after being dried until their weight (W_1) remained constant. Then, the samples' mass suspended in water was calculated (W_2). Then, the pieces were taken out of the water. Finally, before weighing them, the water on the surface was quickly blotted with a paper towel (W_3). The following three equations were then used to determine the samples' water absorption, apparent porosity, and bulk density values [29].

- Water adsorption (%) = $((W_3 - W_1)/W_1) \times 100$
- Apparent porosity (%) = $((W_3 - W_1)/(W_3 - W_2)) \times 100$
- Bulk density (%) = $((W_1)/(W_1 - W_2)) \times 100$

Compressive strength was measured using an Instron 3369 apparatus with a load and loading speed of 50 kN and 0.1 mm/min, respectively, and the pellet size was 13 mm × 17 mm. The morphology and microstructure of the membranes were analyzed using the Hitachi SC 2500 scanning electron microscope (Hitachi High-Technologies Corporation, Japan). An acceleration voltage of 5 kV was used for this examination.

Filtration (permeability of membrane)

The laboratory-scale frontal filtration pilot comprises three components: a 300 mL supply tank, an air compressor, and a pressure gauge. The pressure gauge regulates the pressure of the fluid on the membrane. Before usage, the membrane was immersed in distilled water for 24 h and then inserted into the membrane housing, which has an effective filtration surface area of 2 cm^2. All filtration experiments were conducted at room temperature.

A membrane's permeability (*P*) is an intrinsic characteristic that depends on its structure. In practical terms, permeability can be defined as the ratio of the permeation flux (*JP*) to the applied pressure (ΔPm) [32].

$$P = \frac{JP}{\Delta Pm}$$

where *P* is the permeability (in L/h m^2 bar), *JP* is the permeation flux (in L/h m^2) and ΔPm is the applied pressure (in the bar).

Result and discussion

Chemical compositions

The chemical compositions of red and gray clay are listed in Table 1. The result of red clay shows that the percentage of SiO_2 is very high compared to the other oxides, representing approximately 52.76% of the total weight. Al_2O_3 is also present in a significant percentage, 17.34%. Fe_2O_3 and CaO are in smaller quantities than SiO_2 and Al_2O_3, each representing approximately 5.95% and 3.84%, respectively. K_2O and Na_2O are also in moderate amounts, representing about 4.72% and 0.42%, respectively. MgO, TiO_2, and P_2O_5 are in smaller quantities, representing less than 3% of the total weight.

Gray clay displays a different chemical composition with a relatively high proportion of SiO_2, 47%. CaO and Al_2O_3 are also in significant quantity, representing approximately 14.16% and 9.5% of the total weight, respectively. The material also contains substantial amounts of Fe_2O_3 and MgO, each comprising around 4% of the total weight. Other oxides, MnO, K_2O, Na_2O, and TiO_2, are in smaller amounts, each comprising less than 1%.

An in-depth reading of the chemical composition shows notable differences between the clay samples "Red" and "Gray" in their oxide percentages. The red clay has a higher ratio of SiO_2, Al_2O_3, Fe_2O_3, K_2O, Na_2O, and a lower percentage of CaO and LOI than gray clay. In contrast, gray clay has higher MgO, TiO_2, and MnO rates. These variations in oxide percentages may be attributed to differences in the two clays' origin, mineralogy, and geological history. In general, by comparing the chemical composition of the two clays, it is possible to identify their distinct characteristics and the potential consequences of these disparities on their properties and uses. For example, red clay's SiO_2/Al_2O_3 ratio is 3.02, while gray clay's is 4.94.

Both percentages are significantly higher than the theoretical value of 1.18 for pure kaolinite. They suggest that both samples contain a significant amount of free quartz, aluminosilicate, and other minerals [9,11]. Finally, the loss on ignition (LOI) percentage represents the weight loss due to removing water, organic matter, and decomposition of carbonates during heating. Red clay has a lower LOI percentage, indicating a lower carbonate and organic matter content than gray clay.

Elemental analysis

Table 2 shows the concentration of three heavy metals, As, Cd, and Pb, measured in the two clays. Red clay has a concentration of 129 ppb for arsenic, 53 ppb for cadmium, and 15 ppb for lead. On the other hand, gray clay has a higher concentration for all three elements, with 172 ppb for arsenic, 41 ppb for cadmium, and 10 ppb for lead. Comparing the two clays, it is clear that gray clay has a much stronger concentration of

Table 2 – Elemental analysis of red and gray clay.

Heavy metals	Red clay (ppb)	Gray clay (ppb)
Arsenic (75As)	129	172
Cadmium (112Cd)	53	41
Lead (207Pb)	15	10

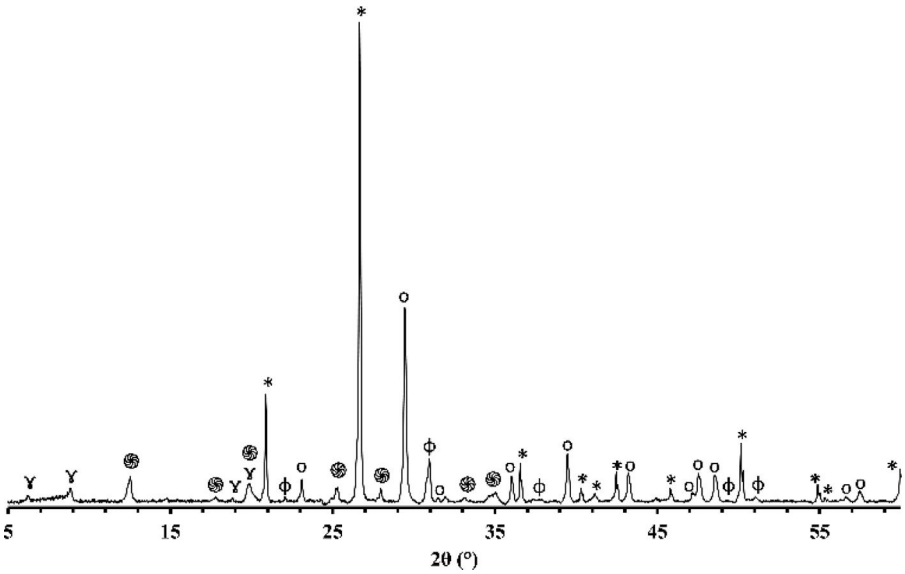

Fig. 1 – XRD patterns of raw gray clay powder. (γ) Montmorillonite; (o) calcite; (*) quartz; (ϕ) dolomite; (γ) talc; (֍) illite.

these. Specifically, gray clay has around 33% higher concentration of arsenic, 22% lower concentration of cadmium, and 31% lower concentration of Lead.

X-ray diffraction (XRD)

Figs. 1 and 2 depict the XRD patterns of red and gray clay powder samples, respectively. Red clay contains minerals, including quartz, calcite, dolomite, hematite, illite, and kaolinite. In contrast, gray clay contains slightly different minerals: quartz, calcite, dolomite, illite, talc, and montmorillonite. These results provide valuable information on the mineralogical characteristics of these two raw clay samples, which may have consequences on their potential use in various industrial and commercial applications. For example, the presence of clay minerals may affect the plasticity and workability of the clay, as well as its firing temperature. Upon meticulous examination of the two diffractograms, the intensity of calcite peaks is clearly greater than that of red clay, which is expected due to the significant proportion of calcium oxide present in the chemical composition of the gray clay. However, despite the red clay containing approximately twice the amount of magnesium oxide, the intensity of the dolomite is considerably weak in contrast to red clay. This phenomenon can be explained by forming another primary phase, talc, by this oxide.

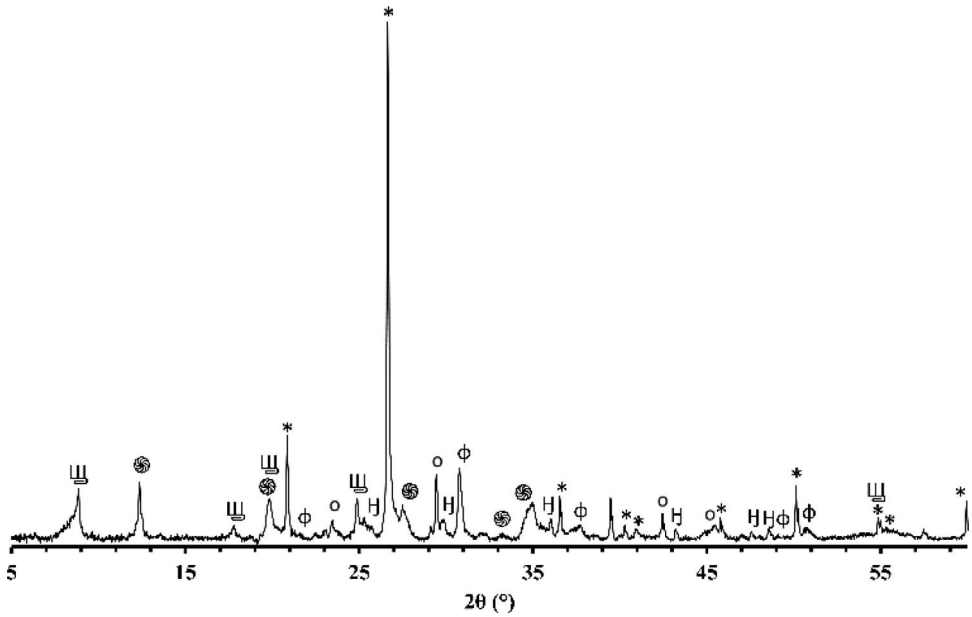

Fig. 2 – XRD patterns of raw red clay powder. (o) Calcite; (*) quartz; (ϕ) dolomite; (֍) illite; (ϑ) hematite; (Ш) kaolinite.

The carbonate content percentage

The differences in carbonate content between the two clays can be explained by the variance in the clays' calcium oxide (CaO) and magnesium oxide (MgO) content. Calcium carbonate ($CaCO_3$) is a principal component of various clays and is often used as an indicator of the clays' overall fertility and productivity. The red clay has a lower carbonate content (4%) than the second clay (16%), implying that the latter possesses a higher concentration of calcium carbonate and dolomite. This deduction is supported by the observation that the gray clay exhibits a considerably higher percentage of CaO (14.16%) than the red clay (3.94%). Magnesium is also noteworthy as it is a significant component of dolomite. The gray clay contains a higher percentage of MgO (4%) than the red clay (2.53%). While the presence of organic matter can influence the carbonate content of clay, it was not considered in this study. This was because the DTA curves of the two clays did not exhibit any exothermic peaks, which would indicate significant thermal decomposition of the organic matter. As a result, the impact of organic matter on the carbonate content was considered negligible for this investigation.

Color of clays

The difference in color between the two clays, red and gray, can be attributed to their mineral compositions. Red clay contains hematite and kaolinite minerals. Hematite is a reddish-brown mineral that gives red clay its reddish hue [33]. Conversely, kaolinite is a white or gray mineral typically not colored, but it can sometimes appear slightly yellow or red [34–37]. Gray clay, on the other hand, contains smectite, montmorillonite, and talc minerals. These minerals do not contain significant amounts of iron oxide like hematite, responsible for the reddish color. Instead, these minerals are gray, which is likely why the clay appears gray [38–40].

Plasticity

The plasticity of clays is primarily determined by mineralogical composition, particle size, particle shape, and water content. However, the chemical composition of the clay also plays a significant role in deciding its plasticity [41]. First, the red clay with a low carbonate content and high Al_2O_3 content has higher plasticity (25%) than the gray clay (15%) with a higher carbonate content and low montmorillonite content. This is because the Al_2O_3 content in the Safi clay can contribute to forming clay minerals, resulting in an increased surface charge and a strong affinity for water molecules, leading to high plasticity. Additionally, the Safi clay's illite and kaolinite clay phases are known to have high plasticity [42]. On the other hand, according to the bibliography, the characteristics of the talc include low specific surface areas. Furthermore, it is generally accepted that the basal surfaces of talc and pyrophyllite are hydrophobic, and the edges are hydrophilic. From these results, it can be inferred that the plasticity of the gray clay is adversely affected by the presence of talc.

Thermal treatment analysis

DTA-TG

Fig. 3 revealed endothermic peaks at different temperatures with corresponding mass loss. The initial peak at 95 °C resulted in a mass loss of about 0.65%, attributed to removing hygroscopic water. A more prominent endothermic peak with a center temperature of 575 °C caused a significant mass loss likely caused by the dehydroxylation of the kaolinite. A small peak observed at 595 °C could be related to the allotropic transformation of quartz. Around 750 °C, the last peak resulted in a significant mass loss and could indicate the calcite's and dolomite's decarbonization. These results suggest that the material undergoes multiple transformations when heated and that each transformation could develop distinct mineralogical phases. The thermal behavior of gray clay (Fig. 4) was similar to that of red clay. Several endothermic peaks were

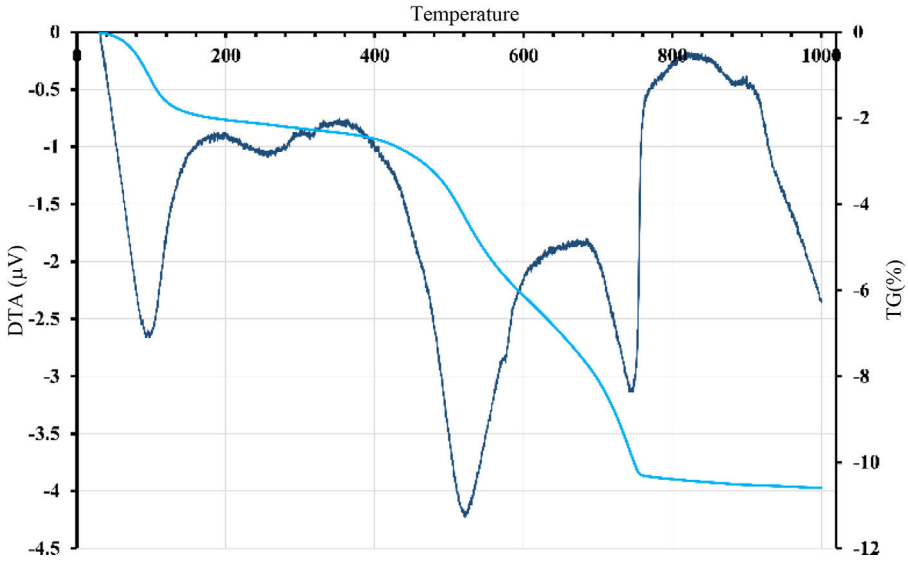

Fig. 3 – DTA-TG curves of red clay.

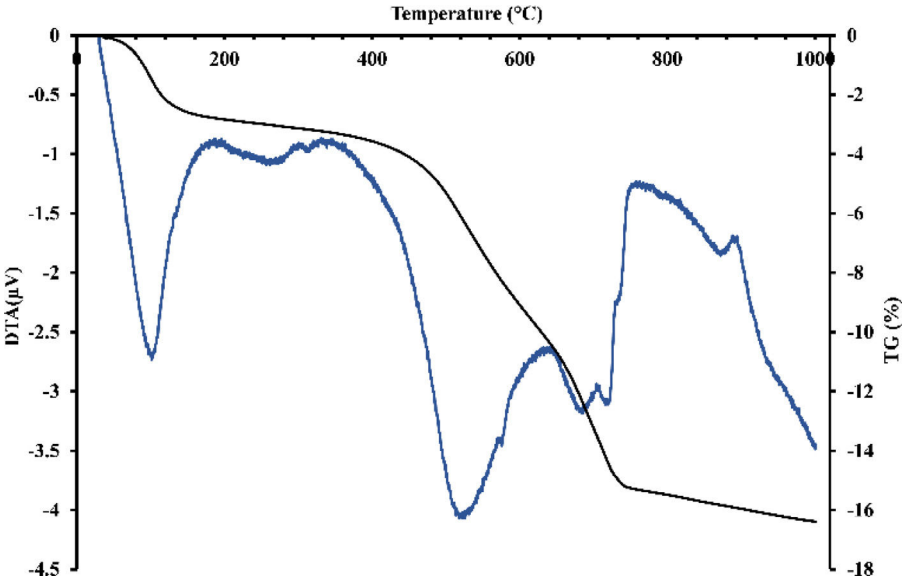

Fig. 4 – DTA-TG curves of gray clay.

observed. The initial peak detected at 95 °C resulted in a mass loss of around 3%, indicating the removal of hygroscopic water. The significant loss in mass is due to smectite, a type of clay mineral with a high surface area that can swell in the presence of water, which can cause a decrease in the bulk density of the material in which it is present.

A larger endothermic peak was observed at 575 °C, resulting in a consequent loss of mass, which could signify the dehydroxylation of smectite, talc, and montmorillonite. Another minor peak was observed at 595 °C, which could be linked to the allotropic transformation of quartz. Finally, the last two peaks, centered around 700 and 750 °C, resulted in significant mass loss, suggesting the decomposition of calcite and dolomite.

Mineralogical transformation

Figs. 5 and 6 show the phases formed during the treatment at different temperatures. These minerals already contain the phases that exist at room temperature, which are calcite ($CaCO_3$), quartz (SiO_2), dolomite ($CaMg(CO_3)_2$), illite ($(K,H_3O)(Al,Mg,Fe)_2(Si,Al)_4O_{10}$), hematite ($Fe_2O_3$), and kaolinite ($Al_2Si_2O_5(OH)_4$). As the temperature increases, various phase transformations occur. At 900 °C, the minerals react to form anorthite ($CaAl_2Si_2O_8$), diopside ($CaMgSi_2O_6$), and gehlinite ($Ca_2Al_2SiO_7$). At 1000 °C, the minerals present at 900 °C continue to form, except for gehlinite ($Ca_2Al_2SiO_7$), which disappears. The evolution of the mineral phases present can be deduced by examining the variation of their intensity on the diffractogram. Gehlinite ($Ca_2Al_2SiO_7$) is a mineral phase

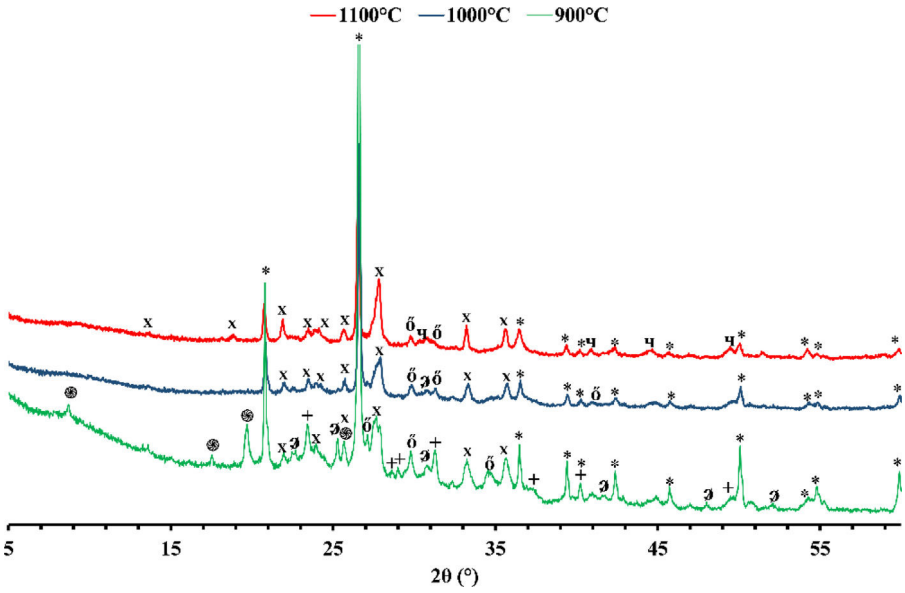

Fig. 5 – XRD patterns of red clay sintered at 900 °C, 1000 °C and 1100 °C. (*) Quartz; (♋) illite; (э) hematite; (X) anorthite; (+) gehlenite; (ő) diopside; (ч) magnetite.

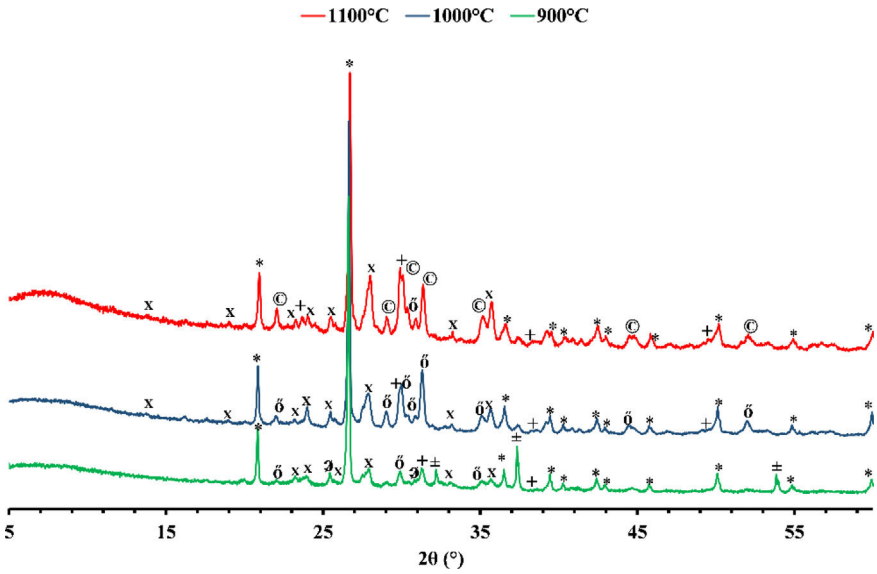

Fig. 6 – XRD patterns of gray clay sintered at 900 °C, 1000 °C and 1100 °C. (*) Quartz; (ϑ) hematite; (X) anorthite; (+) gehlenite; (ő) diopside; (±) CaO; (©) augite.

that forms at around 900 °C, as shown in Table 3. However, it is not present at 1000 °C. This is because, at 1000 °C, the $Ca_2Al_2SiO_7$ phase undergoes a phase transformation into the $CaAl_2Si_2O_8$ phase when there is a substantial amount of free quartz [11,18].

Finally, when red clay is subjected to a temperature of 1100 °C, some minerals undergo significant changes. However, few transformations occur, except for the appearance of a new phase, magnetite (Fe_3O_4), and the disappearance of hematite. The intensity of anorthite increases while that of quartz decreases.

Gray clay is a complicated mixture of several materials at room temperature, including calcite ($CaCO_3$), quartz (SiO_2), dolomite [$CaMg(CO_3)_2$], smectite [$(Na,Ca)_{0.33}(Al,Mg)_2(Si_4O_{10})(OH)_2{\cdot}nH_2O$], illite [$(K,H_3O)(Al,Mg,Fe)_2(Si,Al)_4O_{10}$], and montmorillonite [$Mg_3Si_4O_{10}(OH)_2$]. At 900 °C, the gray clay is primarily composed of quartz (SiO_2), hematite (Fe_2O_3), and a range of high-temperature minerals that form through the decomposition of illite and calcite. The decomposition of illite can result in feldspars, such as $CaAl_2Si_2O_8$ and $KAlSi_3O_8$, while calcite decomposition can lead to wollastonite formation ($CaSiO_3$) and lime (CaO). By heating clay minerals to tem-

Table 3 – Minerals transformation after thermal treatment.

Treatment temperature	Red clay	Gray clay
Ambient	Calcite ($CaCO_3$) Quartz (SiO_2) Dolomite ($CaMg(CO_3)_2$) Illite ($(K,H_3O)(Al,Mg,Fe)_2(Si,Al)_4O_{10}$) Hematite ($Fe_2O_3$) Kaolinite ($Al_2Si_2O_5(OH)_4$)	Calcite ($CaCO_3$) Quartz (SiO_2) Dolomite ($CaMg(CO_3)_2$) Smectite ($(Na,Ca)_{0.33}(Al,Mg)_2(Si_4O_{10})(OH)_2{\cdot}nH_2O$) Illite ($(K,H_3O)(Al,Mg,Fe)_2(Si,Al)_4O_{10}$) Montmorillonite ($Mg_3Si_4O_{10}(OH)_2$)
900 °C	Quartz (SiO_2) Hematite (Fe_2O_3) Anorthite ($CaAl_2Si_2O_8$) Diopside ($CaMgSi_2O_6$) Gehlinite ($Ca_2Al_2SiO_7$)	Quartz (SiO_2) Hematite (Fe_2O_3) Lime (CaO) Wollastonite ($CaSiO_3$) Anorthite ($CaAl_2Si_2O_8$) Diopside($CaMgSi_2O_6$)
1000 °C	Quartz (SiO_2) Hematite (Fe_2O_3) Anorthite ($CaAl_2Si_2O_8$) Diopside ($CaMgSi_2O_6$)	Quartz (SiO_2) Hematite (Fe_2O_3) Anorthite ($CaAl_2Si_2O_8$) Diopside ($CaMgSi_2O_6$)
1100 °C	Quartz (SiO_2) Anorthite ($CaAl_2Si_2O_8$) Diopside ($CaMgSi_2O_6$) Magnetite (Fe_3O_4)	Quartz (SiO_2) Augite ($Ca(Mg, Fe)Si_2O_6$) Anorthite ($CaAl_2Si_2O_8$) Gehlenite ($Ca_2Al_2SiO_7$)

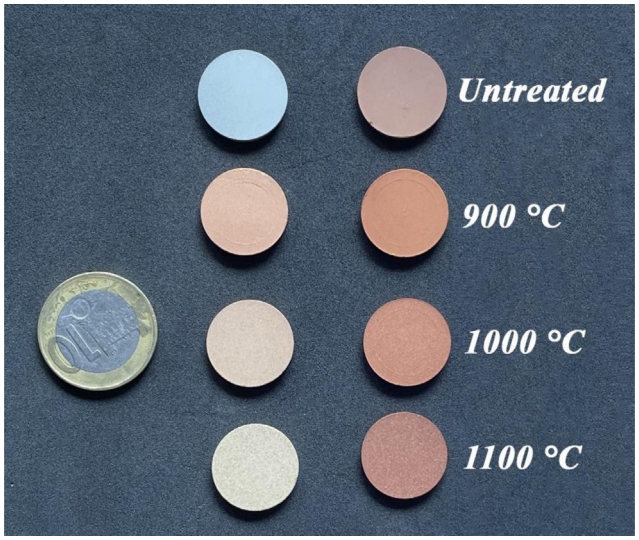

Fig. 7 – Color change of ceramic membranes sintered at different temperatures.

Fig. 8 – Appearance of clay pellets after thermic treatment at 1170 °C.

peratures above 1000 °C, these minerals can develop through high-temperature processes like pyro-metamorphism. These minerals can arise via the recrystallization of clay minerals at high temperatures or from the disintegration of pre-existing minerals like feldspars and pyroxenes. Quartz (SiO_2), hematite (Fe_2O_3), and a variety of high-temperature minerals, such as anorthite ($CaAl_2Si_2O_8$), diopside ($CaMgSi_2O_6$), and gehlenite ($Ca_2Al_2SiO_7$), make up the majority of the gray clay at 1000 °C. When the temperature increases to 1100 °C, the diffractogram shows no significant alterations, indicating that anorthite and gehlinite remain in the dominant phases. However, diopside transforms and is converted into augite $Ca(Mg,Fe)Si_2O_6$ through the process of Mg substitution by Fe. This change in mineral composition can be attributed to the high-temperature conditions.

Color change and fusion test

Fig. 7 illustrates how temperature and mineral transformations influence the color of ceramic membranes. The red clay color variations provide insights into the behavior of the illite mineral under different heating conditions. When exposed to 900 °C, the illite mineral breaks down, releasing iron oxide [11]. This process results in a brick-red hue that remains even when the temperature is raised to 1000 °C. Interestingly, at 1000 °C, the iron oxide does not undergo significant changes, and the brick-red hue remains unchanged. However, when the temperature is increased to 1100 °C, the iron oxide undergoes an oxidation process, leading to the formation of magnetite. The creation of magnetite gives the material a brown hue distinct from the original brick-red color.

The color of the sample is gray at room temperature. However, as the sample was heated to 900 °C, the color changed to brick red, which was attributed to the release of iron oxide resulting from the decomposition of illite. No significant transformation was observed for iron oxide when the temperature was increased to 1000 °C. However, at 1100 °C, the sample turned yellow due to the reaction of hematite, resulting in the formation of augite. These results suggest that mineral composition changes can cause significant alterations in a sample's color.

After subjecting red clay with 3.84% CaO and gray clay with 14.16% CaO to heat treatment at 1170 °C, noticeable differences were observed in Fig. 8. While the gray clay was completely melted, the red clay remained intact, and the pellet appeared to retain its original shape. This suggests that a higher calcium oxide (CaO) content in the gray clay caused it to melt under the given temperature. In contrast, the red clay, with a lower CaO content, displayed greater resistance to the heat and maintained its form [43].

Membranes tests

Figs. 9–11 provide data on various properties measured at different temperatures for two types of clays: red and gray. The properties include open porosity, water absorption, and bulk density. The open porosity of both red and gray clays was measured at three different temperatures: 900 °C, 1000 °C, and 1100 °C.

At 900 °C, the red clay exhibited an open porosity of 28%, while the gray clay had a slightly higher open porosity of 35%. When the temperature was increased to 1000 °C, the open porosity decreased for both materials, with the red clay showing a value of 28% and the gray clay measuring 33%. At the highest temperature of 1100 °C, the red clay's open porosity dropped to 18%, while the gray clay maintained a value of 30%. Similarly, the water absorption was assessed under an identical set of three temperatures. When exposed to a temperature of 900 °C, the red clay exhibited a water absorption rate of 15%, whereas the gray clay displayed a slightly higher absorption rate of 19%. As the temperature increased to 1000 °C, the water absorption of the red clay decreased to 14%, while the gray clay experienced a reduction to 18%. Finally, at the highest temperature of 1100 °C, the water absorption of the red clay plummeted to 9%, while the gray clay maintained a value of 17%.

Furthermore, the bulk density was assessed. At 900 °C, the red clay exhibited a bulk density of 2.68, whereas the gray clay

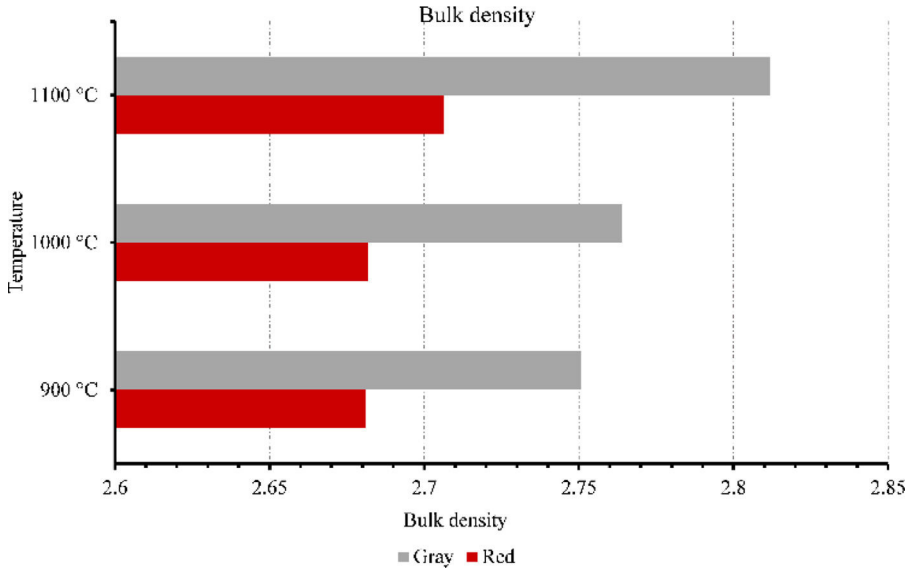

Fig. 9 – Bulk density of membranes firing at 900 °C, 1000 °C and 1100 °C.

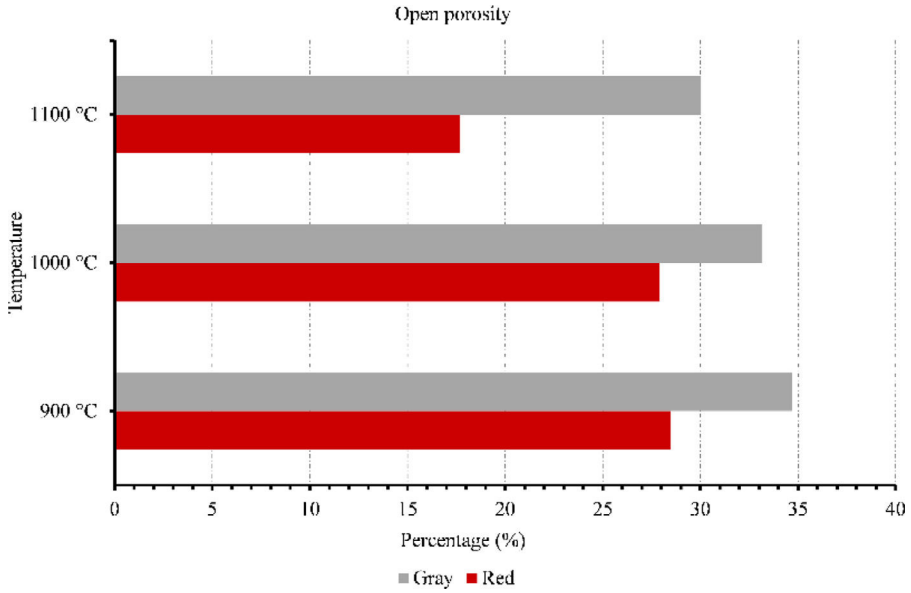

Fig. 10 – Open porosity of membranes firing at 900 °C, 1000 °C and 1100 °C.

had a slightly higher value of 2.75. The bulk density remained relatively consistent as the temperature increased to 1000 °C, with the red clay maintaining a measurement of 2.68 and the gray clay showing a value of 2.76. However, when the temperature reached 1100 °C, both clays experienced a slight increase in bulk density, with the red clay measuring 2.70 and the gray clay measuring 2.81. It can be observed that the gray clay consistently had higher bulk density values compared to the red clay across all three temperatures. At 900 °C, the difference was minimal, with the gray clay having a slightly higher bulk density. However, as the temperature increased to 1100 °C, the disparity in bulk density between the two clays became more pronounced, with the gray clay exhibiting a significantly higher value of 2.81 compared to the red clay's 2.70. This suggests that the gray clay may have a higher packing density or more excellent compaction at elevated temperatures than the red clay.

Both the mineral composition of the ceramic pastes and the optimum firing temperature play a crucial role in determining the efficiency of filtration membranes. These two factors influence the formation of pores in the membrane structure, which has a direct impact on its porosity and, consequently, on its filtration efficiency. At lower firing temperatures, the presence of carbonates and pore formation are closely linked. Carbonation can break down during firing, releasing gases that create pores in the ceramic matrix. Furthermore, pore-forming mechanisms such as sintering and phase transformations are influenced by firing temperature and mineralogical composition. However, at higher firing temperatures, the behavior changes. As temperature increases,

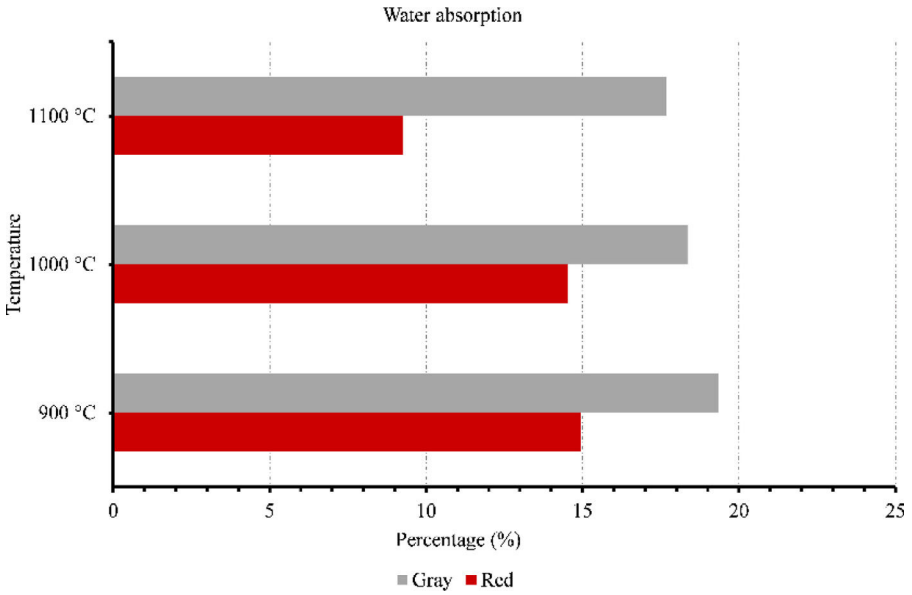

Fig. 11 – Water absorption of membranes firing at 900 °C, 1000 °C and 1100 °C.

ceramic materials undergo vitrification, where pores can be filled with glassy phases, resulting in a decrease in porosity. This is due to the densification of the ceramic structure during sintering, which leads to pore closure or consolidation.

Overall, these results highlight the variations in bulk density, water absorption, and open porosity between red and gray clays at different temperatures, which indicate differences in their structural characteristics and responses to temperature changes. This result will influence their mechanical strength as well as their filtering capacity.

Compressive strength

The compressive strength of ceramic membranes made from red and gray clay was investigated at different temperatures. The results reveal interesting trends regarding the mechanical properties of these membranes (Fig. 12).

Starting with the red clay ceramic membrane, its compressive strength was 60.97 MPa at 900 °C. As the temperature increased to 1000 °C, there was a notable improvement in the compressive strength, which rose to 83.25 MPa. The red clay membrane reached its highest compressive strength at 1100 °C, measuring 110.165 MPa. These findings indicate that as the temperature increased, the red clay ceramic membrane significantly enhanced its structural integrity and ability to withstand compressive forces. In contrast, the gray clay ceramic membrane displayed a different pattern in terms of compressive strength. At 900 °C, its compressive strength was measured at 38.33 MPa, lower than that of the red clay membrane. As the temperature increased to 1000 °C, the gray

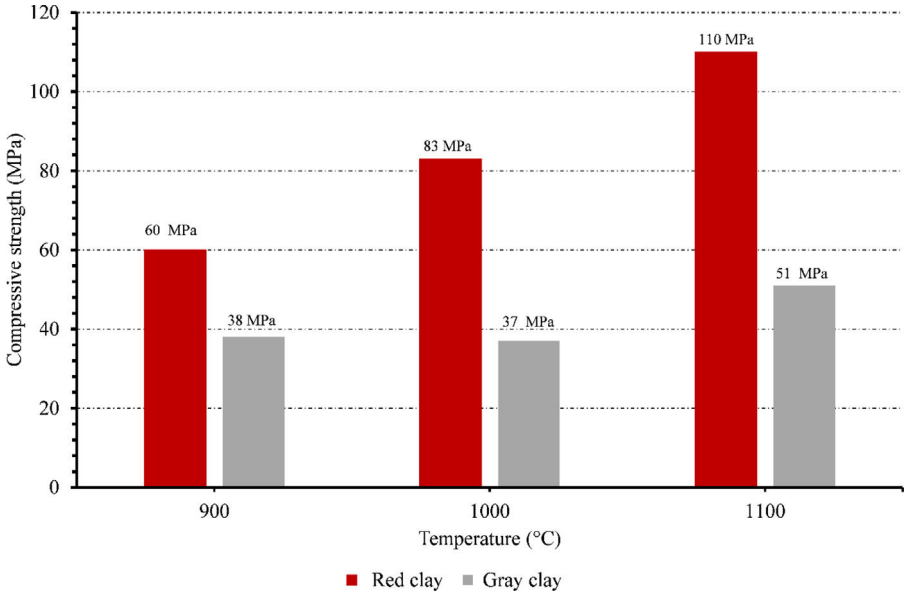

Fig. 12 – Compressive strength of ceramic membranes at different temperatures.

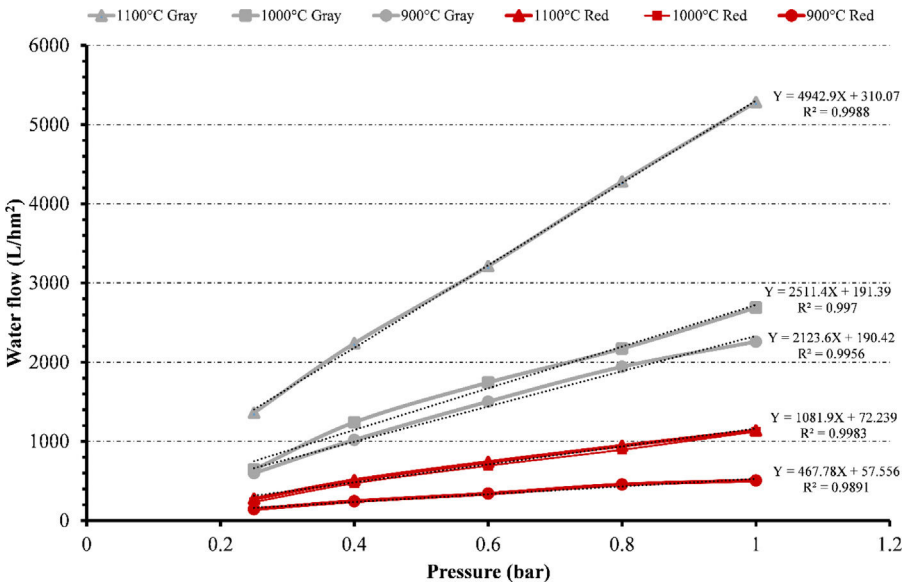

Fig. 13 – Variation in water flux a function of pressures at 900 °C.

clay membrane experienced a slight decrease in compressive strength, measuring 37.925 MPa. However, at 1100 °C, the gray clay ceramic membrane demonstrated a moderate improvement, reaching a compressive strength of 51.155 MPa.

The red clay ceramic membrane consistently outperformed the gray clay membrane in terms of compressive strength throughout all temperature ranges, as can be seen from comparing the two types of membranes. Accordingly, it can be inferred that the red clay ceramic membrane has higher mechanical qualities and is more appropriate for uses requiring excellent resistance to compressive forces.

Water flux

Fig. 13 summarizes the flux values for gray and red clays at different temperatures (900 °C, 1000 °C and 1100 °C) and pressures (ranging from 0.25 to 1 bar). Increased pressure results in higher flux values for both clays at different temperatures. The values obtained for gray clay are always higher than those obtained for red clay.

At 900 °C, the gray flux ranges from approximately 598 L/h m^2 at 0.25 bar pressure to 2260 L/h m^2 at 1 bar pressure. The corresponding red flux ranges from 144 L/h m^2 to 506 L/h m^2. For 1000 °C, the gray flux varies from around 643 L/h m^2 to 2689 L/h m^2 as the pressure increases from 0.25 to 1 bar. The red flux ranges from 233 L/h m^2 to 1123 L/h m^2. At 1100 °C, the gray flux ranges from 1362 L/h m^2 to 5283 L/h m^2, while the red flux ranges from 274 L/h m^2 to 1138 L/h m^2.

Despite the high-temperature heat treatment at 1100 °C, the membrane's permeability still increases. This can be attributed to several factors. Firstly, creating larger pores than those formed at 900 °C contributes to the increased permeability.

These larger pores allow easier water passage and enhance the membrane's permeability. Secondly, although the overall porosity decreases with the high-temperature treatment, the distribution of pores across the membrane is not uniform. Some areas may have a higher concentration of pores, leading to localized regions of increased permeability. This uneven distribution of pores can contribute to the overall permeability increase despite the decrease in porosity.

In conclusion, the combination of larger pore creation, uneven pore distribution, decreased porosity, and improved compression resistance due to well-sintered ceramic surfaces

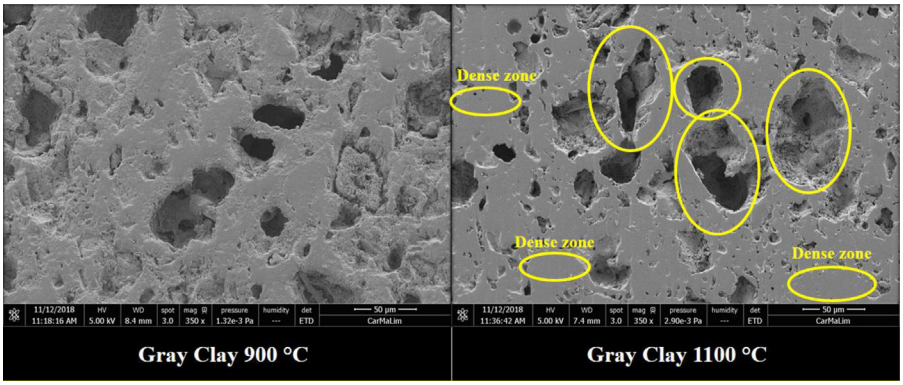

Fig. 14 – SEM image of gray clay after sintering at 900 °C and 1100 °C.

collectively contribute to the overall increase in permeability despite the high-temperature heat treatment at 1100 °C.

The SEM figure provides visual evidence that supports the previously mentioned findings. When clay is sintered at 900 °C, it exhibits a homogeneous pore distribution with small pore sizes that do not exceed a few micrometers. On the other hand, when the membrane is sintered at 1100 °C, it shows a significantly different pore structure. The pore size increases significantly to approximately 25 μm, and the pore distribution becomes uneven, leading to dense and well-compacted zones.

This observation from the SEM image Fig. 14 aligns with the measured permeability results. The smaller pore sizes and homogeneous pore distribution in the clay sintered at 900 °C would contribute to a lower permeability, indicating a more restricted flow of substances through the membrane. In contrast, the larger pore sizes and inhomogeneous pore distribution in the membrane sintered at 1100 °C would result in higher permeability, allowing for easier passage of substances through the membrane.

Therefore, the SEM image confirms that the observed permeability results are consistent with the pore structures at different sintering temperatures.

Conclusion

In conclusion, our research has demonstrated that the two types of membranes exhibit different thermal behaviors. However, based on the obtained results, it is evident that thermal treatment can strongly influence the filtration efficiency of the membrane. Specifically, gray clay can be utilized for selective filtration at low temperatures and in uniformly sized pores.

This conclusion highlights the importance of considering thermal conditions in designing and utilizing filtration membranes. Modifying the thermal treatment parameters makes it possible to optimize the membrane's efficiency and tailor its filtration behavior to meet specific application requirements.

Our findings offer good insights for developing advanced and efficient filtration membranes. They pave the way for future research to refine thermal treatment processes and further explore the selective capabilities of gray clay-based membranes in other application domains. In summary, our study underscores the significance of considering thermal treatment as a key parameter in optimizing the performance of filtration membranes.

The results reinforce that gray clay can be successfully employed for selective filtration at low temperatures and with uniformly sized pores. These conclusions hold promise for advancing research in filtration membranes and their application in various industrial sectors.

Funding

The authors declare that no funds, grants, or other support were received during the preparation of this manuscript.

Competing interests

The authors have no relevant financial or non-financial interests to disclose.

REFERENCES

[1] L. Daoudi, E.H. Elboudour, L. Saadi, A. Albizane, J. Bennazha, M. Waqif, M. Elouahabi, N. Fagel, Characteristics and ceramic properties of clayey materials from Amezmiz region (Western High Atlas, Morocco), Appl. Clay Sci. 102 (2014) 139–147, http://dx.doi.org/10.1016/j.clay.2014.09.029.

[2] T. Hosni, L. Daoudi, T. Remmal, H. El Boudour El Idrissi, M. El Ouahabi, N. Fagel, Influence of the clay composition on the quality of traditional ceramics: example of the site of Mzouda (Central Morocco), Arab. J. Geosci. 14 (2021) 2805, http://dx.doi.org/10.1007/s12517-021-09018-7.

[3] A. Manni, A. El Haddar, I. El Amrani El Hassani, A. El Bouari, C. Sadik, Valorization of coffee waste with Moroccan clay to produce a porous red ceramics (class BIII), Bol. Soc. Esp. Cer. Vid. 58 (2021) 211–220, http://dx.doi.org/10.1016/j.bsecv.2019.03.001.

[4] A. Mellaikhafi, A. Tilioua, H. Souli, M. Garoum, M.A. Alaoui Hamdi, Characterization of different earthen construction materials in oasis of south-eastern Morocco (Errachidia Province), Case Stud. Constr. Mater. 14 (2021) 2214–5095, http://dx.doi.org/10.1016/j.cscm.2021.e00496.

[5] A. Manni, A. Elhaddar, A. El Bouari, I. El Amrani El Hassani, C. Sadik, Complete characterization of Berrechid clays (Morocco) and manufacturing of new ceramic using minimal amounts of feldspars: economic implication, Case Stud. Constr. Mater. 7 (2017) 144–153, http://dx.doi.org/10.1016/j.cscm.2017.07.001.

[6] D. El Machtani Idrissi, Z. Chafiq Elidrissi, B. Achiou, M. Ouammou, S.A. Younssi, Fabrication of low-cost kaolinite/perlite membrane for microfiltration of dairy and textile wastewaters, J. Environ. Chem. Eng. 11 (2023) 2213–3437, http://dx.doi.org/10.1016/j.jece.2023.109281.

[7] G. El Boukili, M. Lechheb, M. Ouakarrouch, A. Dekayir, F. Kifani-Sahban, A. Khaldoun, Mineralogical, physico-chemical and technological characterization of clay from Bensmim (Morocco): suitability for building application, Constr. Build. Mater. 280 (2021), http://dx.doi.org/10.1016/j.conbuildmat.2021.122300, 0950-0618.

[8] M. El Ouahabi, H. El Boudour El Idrissi, L. Daoudi, M. El Halim, N. Fagel, Moroccan clay deposits: physico-chemical properties given provenance studies on ancient ceramics, Appl. Clay Sci. 172 (2019) 65–74, http://dx.doi.org/10.1016/j.clay.2019.02.019.

[9] L. Mérai, Á. Deák, M.A. Harech, M. Abdelghafour, D. Sebők, Á. Ágoston, S.P. Tallósy, T. Szabó, Y. Abouliatim, M. Mesnaoui, L. Nibou, Á. Kukovecz, L. Janovák, Antimicrobial ceramic foam composite air filter prepared from Moroccan red clay, phosphate sludge waste, and biopolymer, Appl. Clay Sci. 230 (2022), http://dx.doi.org/10.1016/j.clay.2022.106703, 0169-1317.

[10] H. Majdoubi, Y. Haddaji, S. Mansouri, D. Alaoui, Y. Tamraoui, N. Semlal, M. Oumam, B. Manoun, H. Hannache, Thermal, mechanical and microstructural properties of acidic geopolymer based on moroccan kaolinitic clay, J. Build. Eng. 35 (2020) 2352–7102, http://dx.doi.org/10.1016/j.jobe.2020.102078.

[11] M.A. Harech, T. Labbilta, Y. Abouliatim, Y. Elhafiane, A. Benhammou, A. Abourriche, A. Smith, L. Nibou, M. Mesnaoui, Influence of thermal treatment of moroccan red clay on its physicochemical and mechanical behavior, Clays Clay Miner. 70 (2022) 601–615, http://dx.doi.org/10.1007/s42860-022-00208-2.
[12] M.M. Jordan, M.A. Montero, E. García-Sánchez, A. Martínez-Poveda, Firing behaviour of tertiary, cretaceous and permo-triassic clays from castellon ceramic cluster (Spain), Appl. Clay Sci. 198 (2020), http://dx.doi.org/10.1016/j.clay.2020.105804.
[13] M.M. Jordán, J.D. Martín-Martín, T. Sanfeliu, D. Gómez-Gras, C. de la Fuente, Mineralogy and firing transformations of Permo–Triassic clays used in the manufacturing of ceramic tile bodies, Appl. Clay Sci. 44 (2009) 173–177, http://dx.doi.org/10.1016/j.clay.2009.01.018.
[14] M.M. Jordan, M.A. Montero, S. Meseguer, T. Sanfeliu, Influence of firing temperature and mineralogical composition on bending strength and porosity of ceramic tile bodies, Appl. Clay Sci. 42 (2008) 266–271, http://dx.doi.org/10.1016/j.clay.2008.01.005.
[15] M.A. Harech, R. Dabbebi, Y. Abouliatim, Y. Elhafiane, A. Smith, M. Mesnaoui, L. Niboue, S. Baklouti, A comparative study of the thermal behaviour of phosphate washing sludge from Tunisia and Morocco, J. Therm. Anal. Calorim. 147 (2022) 5677–5686, http://dx.doi.org/10.1007/s10973-021-10936-7.
[16] D. Hradil, T. Grygar, J. Hradilová, P. Bezdička, Clay and iron oxide pigments in the history of painting, Appl. Clay Sci. 22 (2023) 223–236, http://dx.doi.org/10.1016/S0169-1317(03)00076-0.
[17] J. Torrent, U. Schwertmann, D.G. Schulze, Iron oxide mineralogy of some soils of two river terrace sequences in Spain, Geoderma 23 (1980) 191–208, http://dx.doi.org/10.1016/0016-7061(80)90002-6.
[18] M.A. Harech, M. Mesnaoui, Y. Abouliatim, Y. EL hafiane, A. Benhammou, A. Abourriche, A. Smith, L. Nibou, Effect of temperature and clay addition on the thermal behavior of phosphate sludge, Bol. Soc. Esp. Cer. Vid. 60 (2020) 194–204, http://dx.doi.org/10.1016/j.bsecv.2020.03.002.
[19] S. Aghris, F. Laghrib, Y. Koumya, S. El Kasmi, M. Azaitraoui, A. Farahi, M. Sajieddine, M. Bakasse, S. Lahrich, M.A. El Mhammedi, Exploration of a new source of sustainable aluminosilicate clay minerals from Morocco: mineralogical and physico-chemical characterizations for clear upcoming applications, J. Inorg. Organomet. Polym. 31 (2021) 2925–2938, http://dx.doi.org/10.1007/s10904-021-01950-1.
[20] A. Elgamouz, N. Tijani, I. Shehadi, K. Hasan, M.A. Kawam, Characterization of the firing behavior of an illite–kaolinite clay mineral and its potential use as membrane support, Heliyon 5 (2019) 2405–8440, http://dx.doi.org/10.1016/j.heliyon.2019.e02281.
[21] M. Monsif, A. Zerouale, N.I. Kandri, M. Mozzon, P. Sgarbossa, F. Zorzi, F. Tateo, S. Tamburini, E. Franceschinis, S. Carturan, R. Bertani, Chemical–physical and mineralogical characterization of ceramic raw materials from Moroccan northern regions: intriguing resources for industrial applications, Appl. Clay Sci. 182 (2019), http://dx.doi.org/10.1016/j.clay.2019.105274, 0169-1317.
[22] A. Harrati, A. Manni, A. El Bouari, I. El Amrani El Hassani, C. Sadik, Elaboration and thermomechanical characterization of ceramic-based on Moroccan geomaterials: application in construction, Mater. Today: Proc. 30 (part 4) (2020) 876–882, http://dx.doi.org/10.1016/j.matpr.2020.04.344.
[23] S. Guzlēna, G. Šakale, S. Čertoks, Clayey material analysis for assessment to be used in ceramic building materials, Proc. Eng. 172 (2017) 333–337, http://dx.doi.org/10.1016/j.proeng.2017.02.031.
[24] S. Barakan, V. Aghazadeh, The advantages of clay mineral modification methods for enhancing adsorption efficiency in wastewater treatment: a review, Environ. Sci. Pollut. Res. 28 (2021) 2572–2599, http://dx.doi.org/10.1007/s11356-020-10985-9.
[25] D.S. Dlamini, J. Li, B.B. Mamba, Critical review of montmorillonite/polymer mixed-matrix filtration membranes: possibilities and challenges, Appl. Clay Sci. 168 (2019) 21–30, http://dx.doi.org/10.1016/j.clay.2018.10.016.
[26] S. Bouzid Rekik, S. Gassara, J. Bouaziz, A. Deratani, S. Baklouti, Development and characterization of porous membranes based on kaolin/chitosan composite, Appl. Clay Sci. 143 (2017) 1–9, http://dx.doi.org/10.1016/j.clay.2017.03.008.
[27] F. Ejaz Ahmed, L. Boor Singh, R. Hashaikeh, A review on electrospinning for membrane fabrication: challenges and applications, Desalination 356 (2015) 15–30, http://dx.doi.org/10.1016/j.desal.2014.09.033.
[28] Z. Ding, J.T. Kloprogge, R.L. Frost, G.Q. Lu, H.Y. Zhu, Porous clays and pillared clays-based catalysts. Part 2. A review of the catalytic and molecular sieve applications, J. Porous Mater. 8 (2001) 273–293, http://dx.doi.org/10.1023/A:1013113030912.
[29] C. Zhao, J. Xue, F. Ran, S. Sun, Modification of polyethersulfone membranes – a review of methods, Prog. Mater. Sci. 58 (2012) 76–150, http://dx.doi.org/10.1016/j.pmatsci.2012.07.002.
[30] S. Farhan Azha, M. Shahadat, I. Suzylawati, S.W. Ali, S. Ziauddin Ahammad, Prospect of clay-based flexible adsorbent coatings as cleaner production technique in wastewater treatment, challenges, and issues: a review, J. Taiwan Inst. Chem. Eng. 120 (2021) 178–206, http://dx.doi.org/10.1016/j.jtice.2021.03.018.
[31] J. Steven, I. Fritz, M. Wendell, Experimental support for a predictive osmotic model of clay membranes, Geochim. Cosmochim. Acta 47 (1983) 1515–1522, http://dx.doi.org/10.1016/0016-7037(83)90310-1.
[32] M.A. Harech, T. Labbilta, I. Anasser, Y. El hafiane, Y. Abouliatim, L. Nibou, A. Smith, M. Mesnaoui, From by-product to sustainable building material: reusing phosphate washing sludge for eco-friendly red brick production, J. Build. Eng. 78 (2023) 2352–7102, http://dx.doi.org/10.1016/j.jobe.2023.107575.
[33] M. Yan, C. Sun, J. Xu, J. Dong, W. Ke, Role of Fe oxides in corrosion of pipeline steel in a red clay soil, Corros. Sci. 80 (2014) 309–317, http://dx.doi.org/10.1016/j.corsci.2013.11.037.
[34] L. Moritz, M. Ralf, Australian sedimentary opal-A and its associated minerals: implications for natural silica sphere formation, Am. Min. 99 (2014) 1488–1499, http://dx.doi.org/10.2138/am.2014.4791.
[35] H. Hong, G.J. Churchman, Y. Gu, K. Yin, C. Chaowen Wang, Kaolinite–smectite mixed-layer clays in the Jiujiang red soils and their climate significance, Geoderma 173–174 (2011) 75–83, http://dx.doi.org/10.1016/j.geoderma.2011.12.006.
[36] P.A. Schroeder, R.J. Pruett, D. Nathan, N.D. Melear, Crystal-chemical changes in an oxidative weathering front in a georgia kaolin deposit, Clays Clay Miner. 52 (2004) 211–220, http://dx.doi.org/10.1346/CCMN.2004.0520207.
[37] C.S. Ross, P.F. Kerr, The clay minerals and their identity, J. Sediment. Res. 1 (1931) 55–65, http://dx.doi.org/10.1306/D4268DC9-2B26-11D7-8648000102C1865D.
[38] C. Viseras, R. Sánchez-Espejo, R. Palumbo, N. Liccardi, F. García-Villén, A. Borrego-Sánchez, M. Massaro, S. Riela, A. López-Galindo, Clays in cosmetics and personal-care products, Clays Clay Miner. 69 (2021) 561–575, http://dx.doi.org/10.1007/s42860-021-00154-5.

[39] V.M. Dekov, J. Cuadros, W.C. Shanks, R.A. Koski, Deposition of talc – kerolite–smectite – smectite at seafloor hydrothermal vent fields: evidence from mineralogical, geochemical and oxygen isotope studies, Chem. Geol. 247 (2008) 171–194, http://dx.doi.org/10.1016/j.chemgeo.2007.10.022.
[40] C. Vogt, J. Lauterjung, R.X. Fischer, Investigation of the clay fraction (<2 μm) of the clay minerals society reference clays, Clays Clay Miner. 50 (3) (2002) 388–400, http://dx.doi.org/10.1346/000986002760833765.
[41] J.F. Burst, The application of clay minerals in ceramics, Appl. Clay Sci. 5 (1991) 421–443, http://dx.doi.org/10.1016/0169-1317(91)90016-3.
[42] R. Habiballah, O. Witam, M. Ibnoussina, M. Duc, Coastal cliff failures hazard along the Safi coastline (Morocco): a methodology for shoreline change assessment and its forecast along with examination of the causes, Environ. Earth Sci. 82 (2023) 255, http://dx.doi.org/10.1007/s12665-023-10925-z.
[43] W. Wang Liang, G. Guang-wei Wang, X. Xiao-jun Ning, J. Jian-liang Zhang, Y. Yan-jiang Li, C. Chun-he Jiang, Effect of CaO mineral change on coal ash melting characteristics, J. Energy Inst. 93 (2019) 642–648, http://dx.doi.org/10.1016/j.joei.2019.06.001.